FORSCHUNGSZENTRUM JÜLICH GmbH

Institut für Plasmaphysik
Association EURATOM-KFA

Interferometric Measurement of the Sawtooth Pre- and Postcursor Oscillations in Ohmic Discharges on TEXTOR

H.R. Koslowski G. Bertschinger G. Fuchs
A. Krämer-Flecken H. Soltwisch

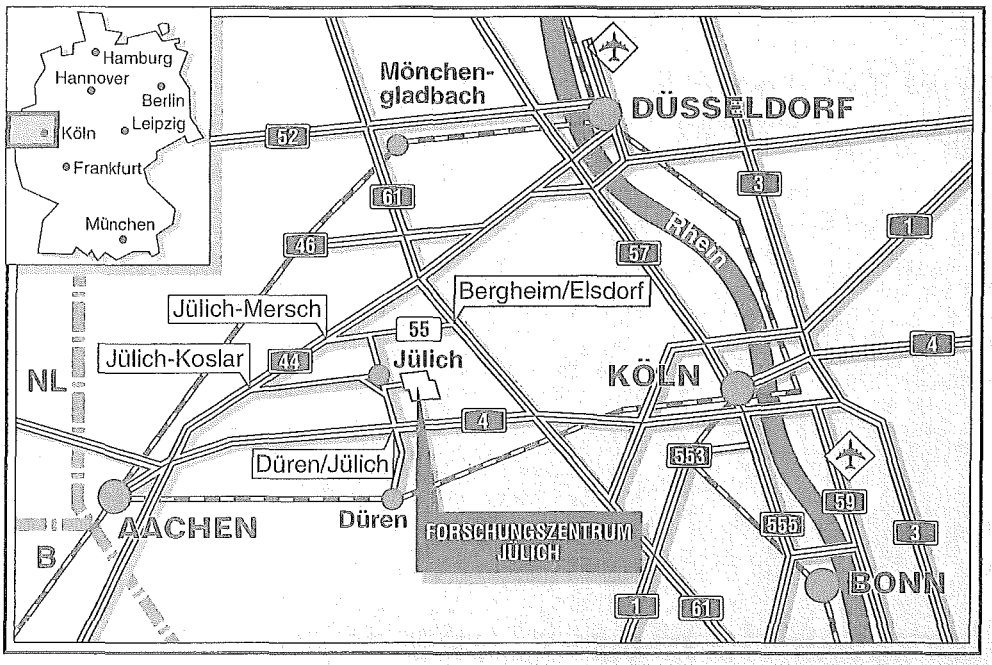

Berichte des Forschungszentrums Jülich ; 3114
ISSN 0944-2952
Institut für Plasmaphysik Jül-3114
Association EURATOM-KFA

Zu beziehen durch: Forschungszentrum Jülich GmbH · Zentralbibliothek
D-52425 Jülich · Bundesrepublik Deutschland
Telefon: 02461/61-6102 · Telefax: 02461/61-6103 · Telex: 833556-70 kfa d

Interferometric Measurement of the Sawtooth Pre- and Postcursor Oscillations in Ohmic Discharges on TEXTOR

H. R. Koslowski G. Bertschinger G. Fuchs
A. Krämer-Flecken H. Soltwisch*

* Institut für Experimentalphysik, Ruhr-Universität Bochum, D-44780 Bochum, Germany

Interferometric Measurement of the Sawtooth Pre– and Postcursor Oscillations in Ohmic Discharges on TEXTOR

H. R. Koslowski, G. Bertschinger, G. Fuchs,
A. Krämer-Flecken, H. Soltwisch*
Institut für Plasmaphysik, Forschungszentrum Jülich GmbH
Ass. EURATOM-KFA, D-52425 Jülich, Germany

Abstract

The sawtooth activity of the electron density and temperature profiles in Ohmic discharges has been investigated in TEXTOR for a wide range of plasma parameters using a nine channel far-infrared interferometer and a ten channel ECE-radiometer. The $m = 1$, $n = 1$ precursor oscillation starts during the last $2 - 3$ ms of the sawtooth ramp-up phase. The frequency slows slightly down while the amplitude increases. The outflow of density is poloidally asymmetric and correlated with the rotation of the helical $m = 1$ perturbation. An oscillation with the same phase and frequency as the precursor which is apparent after the crash contradicts the full reconnection model.

*Institut für Experimentalphysik, Ruhr-Universität Bochum, D-44780 Bochum, Germany

1 Introduction

The sawtooth activity of tokamak discharges is still an unresolved issue in the field of nuclear fusion research. In the past years many experimental observations have been reported questioning the long-standing assumption of full reconnection which was put forward by Kadomtsev [1] shortly after the first report of the sawtooth-like modulation of the soft X-ray radiation from the plasma core in the ST tokamak [2]. Some of these are the existence of postcursor oscillations [3, 4, 5, 6], the growth rate of the sawtooth instability, the timescale on which the sawtooth collapse occurs [7, 8], and measurements of the central safety factor [9, 10, 11, 12], giving values below one during the whole sawtooth period.

Most of the experimental work on sawtooth activity is based on the analysis of the soft X-ray emission being a well established diagnostic on most tokamaks. A drawback of this method is, that the measured emission from the plasma is a function of the electron density, the electron temperature and the impurity concentration, thus making the interpretation of the data difficult. Extreme examples are given in refs. [5, 13] where the SXR-emission from the center of the plasma shows inverted sawteeth due to impurity injection but the electron temperature as measured by ECE radiation remains unaffected. The SXR-emission is found to correlate well with the electron temperature in Ohmic heated discharges but the relation becomes much more difficult when additional heating by ECRH is applied [14]. Further problems for the interpretation arise from the tomographic methods used to evaluate the local emission. Depending on the number of viewing angles analyzed this can lead to ambiguous results even for the same data set [15].

In the following we present measurements of the line-average electron density and the electron temperature during the sawtooth crash in Ohmic heated discharges made with the nine-channel far-infrared interferometer and the ECE-radiometer system installed on TEXTOR. The analysis is based on the raw data and does not require assumptions on the contour line structure of the plasma as no inversion procedure is involved. The time resolution of both measurements has been chosen high enough to resolve details of the fast crash phase.

The experimental investigation was stimulated by the question whether the precursor oscillation and the sawtooth crash exhibit a fixed phase relation.

2 Experiment

The TEXTOR tokamak has a major radius of 1.75 m. The minor plasma radius as determined by the toroidal belt limiter ALT-II is $r = 0.46$ m. The toroidal magnetic field amounts to 2.25 T. The sawtooth activity has been investigated in Deuterium-fueled Ohmic discharges at plasma currents between 250 kA and 500 kA and line-average electron densities between 2×10^{13} cm^{-3} and 4×10^{13} cm^{-3}. The central electron temperature was in the range from 800 eV to 1.2 keV, the effective charge number in this series of discharges was below 2. Under these discharge conditions the magnetic axis was located at about $R = 1.80$ m. A far-infrared interferometer measures the line-integrated electron densities along nine vertical chords at different major radii in one poloidal cross-section of the plasma. An ECE-radiometer measures the local electron temperature at ten radial positions in the equatorial plane of the torus.

The two central probing beams of the interferometer at major radii of 1.75 m and 1.85 m intersect the $q = 1$ surface at the high-field side (HFS) and low-field side (LFS), respectively. Two other probing beams at 1.65 m and 1.95 m are located on the HFS and LFS outside of the sawtooth inversion radius, close to the $q = 1$ surface. Both central beams are modulated due to the rotation of a $m = 1$ precursor mode, whereas the channels outside of the inversion radius show under normal discharge conditions no precursor oscillation, but detect the inverted sawteeth.

Both diagnostics, the ECE-radiometer and the HCN-interferometer, are located at opposite toroidal positions (i.e. their distance is half the long way around the torus).

The amplitude of the sawtooth measured on the central channels of the interferometer is about one tenth of an interference fringe corresponding to $\int n_e dl = 6.6 \times 10^{14}$ cm^{-2}. The noise on the signals is in the order of 1/100 of a fringe. For further noise reduction the high reproducibility of the sawteeth during the flat-top phase of the discharge allows the application of a coherent signal averaging technique [16] with respect to the sawtooth crash. The times for every individual sawtooth crash are determined from either the measurement of the central line integrated density or from the ECE measurement of the central electron temperature as explained in more detail below.

3 Noise reduction technique

The time trace of the signal to be averaged $s(t)$ is divided into intervals with a length of about two sawtooth periods, centered around the sawtooth

crash times $t_1 \ldots t_N$, where N is the number of sawteeth detected during the flat-top phase of the discharge. Each interval contains $2M + 1$ sampling points s_k $(k = I(t_i) - M \ldots I(t_i) + M)$, with $I(t_i)$ being the array index corresponding to the sawtooth crash time t_i, and M is suitably chosen to cover about one mean sawtooth period. These intervals are averaged by calculating the average value for each sample point $\overline{s_k} = N^{-1} \sum_{i=1}^{N} s_{I(t_i)+k}$.

The coherent averaging of a signal has the following properties: Signal features which are randomly distributed with respect to the crash times t_i (i.e. which have a random time difference, as for example noise) are damped in amplitude. For purely statistical noise this damping is by a factor $\sqrt{N}$. On the other hand, signal features which exhibit a constant phase remain nearly undamped in amplitude. (A slight decrease of the amplitude of such features results as a consequence of the finite sampling of the signals.)

We apply different numerical algorithms to detect the sawtooth crash, they work as follows:

1) The signal which is chosen to provide the *sawtooth clock* is *differentiated* with respect to time. The derivative shows negative spikes if the signal has normal sawteeth and positive spikes if the signal has inverted sawteeth. We take the spikes which exceed a certain *threshold level* and identify the sawtooth crash time with the time when these spikes reach their maximum negative or positive value, respectively. Thus the procedure does not give the starting time of the sawtooth collapse but the time when the signals have their *largest rate of change*. The resulting time jitter is in the order of the sampling period because the sawteeth are highly reproducible. The procedure gives a sufficiently stable sawtooth trigger when the reference signal shows only little or no precursor activity. In order to make the algorithm work even when the signal does have precursor oscillations, the following constraint has to be fulfilled: a spike on the differentiated signal is only accepted to be a sawtooth crash when there follows no second spike within a time interval smaller than the precursor period.

2) The signal from which the sawtooth collapse times are determined can be preprocessed with a bandpass filter. The filter applied is a very steep digital FIR filter [17] with a stopband attenuation of more than 60 dB. Full attenuation is reached within less than one octave from the corner frequencies. Bandpass filtering the sawtooth reference signal (the corner frequencies were chosen to be 400 Hz and 800 Hz, respectively; the precursor frequency is about 3 kHz) transforms the sawtooth crash into a typical bipolar pulse shape whose zero-crossing is taken as the crash time.

3) Furthermore we have applied the method of singular value decomposition (SVD) [18] to the data from the nine-channel HCN-interferometer. SVD decomposes a two-dimensional set of spatial and temporal measurements

into an orthonormal basis of radial profiles and the corresponding temporal evolutions of these [19]. The first three radial eigenfunctions of the interferometric data are typically the mean profile of the line integrated electron density, and two functions describing the sawtooth crash and the $m = 1$ precursor oscillation. The time evolution of the sawtooth eigenfunction can be used to provide the sawtooth reference. The determination of the crash times is then not influenced by the precursors because they are described by another eigenfunction. Thus straightforward differentiation of the sawtooth time trace gives an excellent sawtooth trigger.

The first method described above resembles the technique of boxcar-averaging. The other methods take advantage of signal processing techniques in the sense, that that signal component whose phase relation with the sawtooth crash is to be checked is effectively suppressed by either filtering in the frequency (ω) domain (FIR bandpass) or filtering in k-space (SVD).

4 Results

4.1 Phase relation between the sawtooth crash and the precursor oscillation

The application of the coherent signal averaging is demonstrated in the following example. Figure 1 shows the line-integrated density at $R = 1.75$ m for a discharge with $I_p = 400\,\mathrm{kA}$ and $\overline{n_e} = 4 \times 10^{13}\,\mathrm{cm}^{-3}$. Due to a high noise level the precursor oscillations during the last 2 ms of the sawtooth ramp-up phase are barely visible. (These measurements suffered from a coating of the tokamak windows which attenuated the probing beam intensity considerably.) The Fourier spectrum of the signal shown in figure 2 shows a peak around 2.8 kHz which indicates the precursor oscillation.

Figure 3 displays the time traces of the sawtooth (a) and the precursor (b) components derived from the SVD. The sawtooth eigenfunction is differentiated in order to derive the sawtooth crash times. The coherent signal averaging of about $N \sim 40$ periods of the precursor signal results in a damping $\propto \sqrt{N}$ of the precursor amplitude (c), proving a random phase between both components.

In order to test this we have applied the bandpass method on the ECE signal from the plasma center for determination of the sawtooth collapse times. After the coherent averaging of the interferometric data we found nearly no remaining precursor oscillation, indicating again a random orientation of the structure when the sawtooth crash appears.

A somewhat surprising result is obtained if we determine the time of the

sawtooth collapse from the central ECE channel by differentiation of the *unfiltered* signal. The result of the superposition of 428 individual sawteeth from the steady state phases of 11 identical discharges is shown in figure 4. As expected, the noise level is strongly decreased, but the amplitude of the precursor shows nearly no damping. The Fourier spectrum (fig. 5) of the coherently averaged signal makes clear that the noise continuum is reduced without affecting the peak at 2.8 kHz.

The finding that the precursor oscillation is not damped by the averaging procedure can only be interpreted in one of the two ways:

- there is a fixed phase relation to the sawtooth crash or
- the applied technique of fixing the sawtooth collapse is not free from picking up information on the phase of the mode oscillation.

Only the method 1, where the crash times are derived by simple differentiation of the (unfiltered!) signal, results in nearly no damping of the amplitude of the precursor modulation. Both other methods applied result in a decrease of the precursor amplitude by the same ratio which one would expect for purely uncorrelated events. As both methods use some sort of filter which is suited to suppress signal features related to the precursor oscillation, we have to conclude that the observed fixed phase relation between the precursor and the sawtooth is a numerical artefact. On the other hand, method 1 can be applied to increase the signal to noise ratio of the signals and offers the possibility to look onto details of the precursor oscillation itself.

Although indications for a fixed phase relation between the precursor oscillation and the sawtooth crash have been reported from SXR-measurements on TEXT [6] and from interferometric measurements on RTP [20], the present results do not confirm these findings.

4.2 Investigation of the precursor oscillations

In the following we apply the differentiation method (1) for coherent signal averaging. The conclusions which will be drawn for the precursor oscillation do not rely on the **absolute** phase with respect to the sawtooth collapse, but only on the **relative** phase between different channels of one diagnostic.

Figure 6 shows the sawtooth averaged signals of the inner four interferometric probing beams. The beams at major radii of $R = 1.75$ m and $R = 1.85$ m show the modulation due to the rotation of the precursor mode with opposite phase. This proves that the toroidal mode number m is at least odd, and a further analysis of SXR signals taken with two cameras in one poloidal cross section yields that m is most likely equal to one.

The precursor period increases from $\tau_{pc} = 330\ \mu$s when the mode starts to 360μs just before the sawtooth crash.

The signals measured at $R = 1.65$ m and $R = 1.95$ m show the inverted sawteeth resulting from the outflow of plasma thereby increasing the density outside of the inversion radius. As seen from figure 6, the inverted sawtooth at $R = 1.65$ m precedes the one at $R = 1.95$ m. The delay between both sides amounts to half of the precursor period. As we will discuss later on, this proofs that the outflow of the plasma during the sawtooth crash is poloidally located. (Note that the applied method of signal averaging projects the $m = 1$ perturbation under investigation into the poloidal plane with an angular orientation which depends on the selected sawtooth trigger signal. Thus the observed inside-outside asymmetry is not a real feature of every individual sawtooth, but reflects the poloidal position of the $m = 1$ structure when the trigger threshold is reached.)

The sawtooth averaged ECE measurement of the electron temperature at various radial positions for the same discharges are plotted in figure 7. In contrast to the density measurement the inverted sawtooth in the electron temperature appears first at $R = 1.91$ m and precedes the one at $R = 1.64$ m. Both measurements demonstrate that the outstreaming of heat and density is coupled to the $m = 1$ precursor mode. The diagnostics for the electron temperature and the electron density are located at toroidally opposite positions. A point of the helical $m = 1$ perturbation which is at the LFS at the location of the ECE diagnostic is at the HFS at the toroidal position of the HCN-interferometer and vice versa.

Figure 8 shows another example of an OH discharge with standard conditions ($\overline{n_e} = 3.1 \times 10^{13}$ cm^{-3}, $I_p = 350$ kA). The signals are averaged over about 40 individual sawtooth events. The ECE signal from the plasma center is plotted in the lower part of the figure. The precursor period is about $360\,\mu$s. The sawtooth collapse is asymmetric with respect to both sides of the plasma center. The inverted sawteeth are modulated by the rotating structure during the crash phase. This supports the previous observation that the outflow of density is poloidally localized at the $q = 1$ surface. The modulation of the inverted sawteeth throughout and after the sawtooth crash as well as a remaining modulation of the central HCN probing beams after the crash with the same frequency as the precursor (the *postcursor oscillation*) are not consistent with the full reconnection model. The postcursor oscillation is not visible on the central electron temperature measurement.

The conventional picture, which is often applied, is, that a crescent shaped $m = 1$ island grows and displaces the plasma core. The electron density and temperature within the island are assumed to be constant or to experience a relatively small change during the growth of the island [21, 22]. The modu-

lation of the line integrated signals can then be interpreted in the following way: when the line of sight crosses the $q = 1$ surface in the vicinity of the plasma core, the signal has a maximum because the density in the plasma core (where most of the beam intersects) is higher than within the flat part of the profile; by contrast the signal shows a minimum when the island has rotated to let the probing beam pass mainly through the flattened part of the profile.

The time traces of the density signals in figure 8 show that the onset of the sawtooth crash (seen by the increasing density at $R = 1.65$ m) coincides with a maximum on the signal measured at $R = 1.75$ m, i.e. when the beam passes mainly through the unmodified part of the electron density profile. Therefore we can conclude that the electrons escape at this poloidal location of the helical $m = 1$ perturbation. (Measurements from TFTR using an ECE imaging technique and X-ray tomography have been interpreted as being indicative of heat outflow through the X-point of the island [23].)

5 Conclusion

The detailed analysis of the sawtooth modulations of the line integrated electron density and the electron temperature in OH discharges in TEXTOR shows that the sawtooth collapse has no unique phase relation to the precursor oscillation. The outflow of electrons and heat during the sawtooth crash is not radially symmetric but is localized somewhere at the circumference of the $q = 1$ surface. The observations are in agreement with all theoretical descriptions of the sawtooth collapse involving some kind of $m = 1$ perturbation, e.g. [24, 25]. The $m = 1$ structure persists during the sawtooth crash and is still present after the collapse as evidenced by postcursor oscillations which is contradictory to the assumption of a full reconnection.

References

[1] Kadomtsev B B 1975 *Sov. J. Plasma Phys.* **1** 389

[2] v Goeler S, Stodiek W and Sauthoff N 1974 *Phys. Rev. Lett.* **33** 1201

[3] Dubois M A, Marty D A and Pochelon A 1980 *Nucl. Fusion* **20** 1355

[4] Westerhof E, Smeulders P and Lopes Cardozo N 1989 *Nucl. Fusion* **29** 1056

[5] Companant la Fontaine A, Dubois M A, Pecquet A L *et al* 1985 *Plasma Phys. Control. Fusion* **27** 229

[6] Snipes J A and Gentle K W 1986 *Nucl. Fusion* **26** 1507

[7] Campbell D J, Gill R D, Gowers C W *et al* 1986 *Nucl. Fusion* **26** 1085

[8] Edwards A W, Campbell D J, Engelhardt W W *et al* 1986 *Phys. Rev. Lett.* **57** 210

[9] Soltwisch H, Stodiek W, Manickam J and Schlüter J 1987 *Proc. 11th Intern. Conf. on Plasma Physics and Contr. Nuclear Fusion Research* (Kyoto) vol. 1 (Vienna: IAEA) 263

[10] O'Rourke J 1991 *Plasma Phys. Control. Fusion* **33** 289

[11] Levington F M, Fonck R J, Gammel G M *et al* 1989 *Phys. Rev. Lett.* **63** 2060

[12] Wróblewski D and Lao L L 1991 *Physics Fluids* **B 3** 2877

[13] Pasini D, Mattioli M, Edwards A W *et al* 1990 *Nucl. Fusion* **30** 2049

[14] Bobrovskij Yu N, Dnestrovskij D A, Kislov D A *et al* 1990 *Nucl. Fusion* **30** 1463

[15] Janicki C, Décoste R and Simm C 1989 *Phys. Rev. Lett.* **62** 3038

[16] Soltwisch H, Fuchs G, Koslowski H R, Schlüter J and Waidmann G 1991 *Proc. 19th Europ. Conf. on Contr. Fusion and Plasma Phys.* (Berlin) vol II p 17

[17] Azizi S A 1981 *Entwurf und Realisierung digitaler Filter* (München: Oldenbourg) 234

[18] Nardone C 1992 *Plasma Phys. Control. Fusion* **34** 1447-65

[19] Fuchs G, Miura Y and Mori M 1994 *Plasma Phys. Control. Fusion* **36** 307

[20] van Lammeren A C A P, Timmermanns J C M, Hogeweij G M D *et al* 1991 *Proc. 19th Europ. Conf. on Contr. Fusion and Plasma Phys* (Berlin) vol II p 73

[21] Dubois M A, Pecquet A L and Reverdin C 1983 *Nucl. Fusion* **23** 147

[22] Hattori K, Cavallo A, Yamada H *et al* 1989 *J. Phys. Soc. Japan* **58** 167

[23] Nagayama Y, McGuire K M, Bitter M *et al* 1991 *Phys. Rev. Lett.* **67** 3527

[24] Rogister A 1991 *Proc. 13th Intern. Conf. on Plasma Physics and Contr. Nuclear Fusion Research* (Washington) vol 2 (Vienna: IAEA) 231

[25] Wesson J A 1990 *Nucl. Fusion* **30** 2545

Figure captions

Figure 1: Line-average electron density at $R = 1.75$ m for a discharge with $I_p = 400$ kA, $\overline{n_e} = 4 \times 10^{13}$ cm^{-3}.

Figure 2: Fourier spectrum of the time trace shown in fig. 1. The peak near 2.8 kHz results from the sawtooth precursor oscillations.

Figure 3: Temporal eigenfunctions of the sawtooth (a) and precursor (b) components derived from singular value decomposition. Curve (c) is the coherently averaged precursor time trace. The amplitude has decreased by a factor $\propto N^{-1/2}$.

Figure 4: Line-average electron density at $R = 1.75$ m after averaging 428 sawteeth (see text).

Figure 5: Fourier spectrum of the averaged signal from fig. 3.

Figure 6: Coherently averaged signals of four interferometric probing beams. The chords at $R = 1.75$ m and $R = 1.85$ m intersect the $q = 1$ surface on both sides of the magnetic axis, the beams at $R = 1.65$ m and $R = 1.95$ m measure outside of the sawtooth inversion radius. The time trace at $R = 1.65$ m sees the inverted sawtooth prior to the one at $R = 1.95$ m.

Figure 7: ECE measurement of the electron temperature (sawtooth averaged). The sawtooth crash starts at $R = 1.91$ m, in contrast to the electron density measurement (fig. 6). As both diagnostics are located at toroidally opposite places, this demonstrates that the outflow of heat and particles is coupled to the $m = 1$ precursor mode.

Figure 8: Sawtooth averaged line-integrated electron densities at various radial positions for a standard OH discharge ($I_p = 360$ kA, $\overline{n_e} = 3.1 \times 10^{13}$ cm^{-3}). The inverted sawtooth at $R = 1.95$ m is delayed by half of the precursor period. The signals are modulated due to the rotating $m = 1$ perturbation throughout and after the sawtooth crash. The modulation after the crash seen by the probing beam at 1.85 m (postcursor-oscillation) amounts to 20% of the maximum precursor modulation. The lower part of the figure shows the central electron temperature which exhibits the precursor oscillations but no postcursor oscillation.

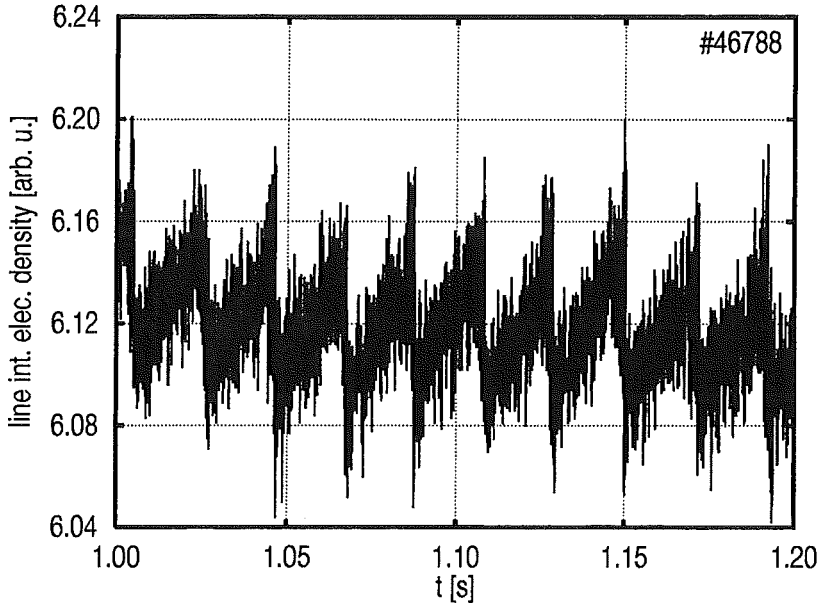
#46788
line int. elec. density [arb. u.]
6.24
6.20
6.16
6.12
6.08
6.04
1.00
1.05
1.10
1.15
1.20
t [s]

Fig. 1

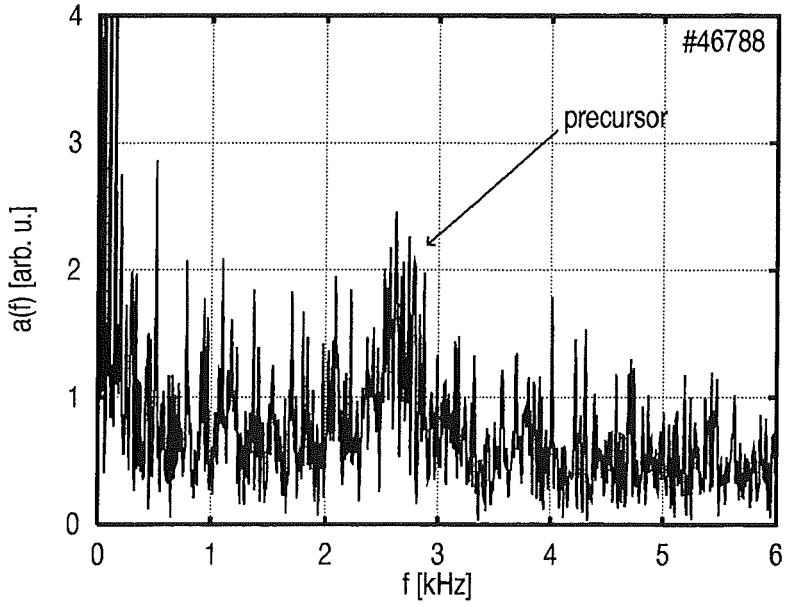
#46788
precursor
a(f) [arb. u.]
4
3
2
1
0
0
1
2
3
4
5
6
f [kHz]

Fig. 2

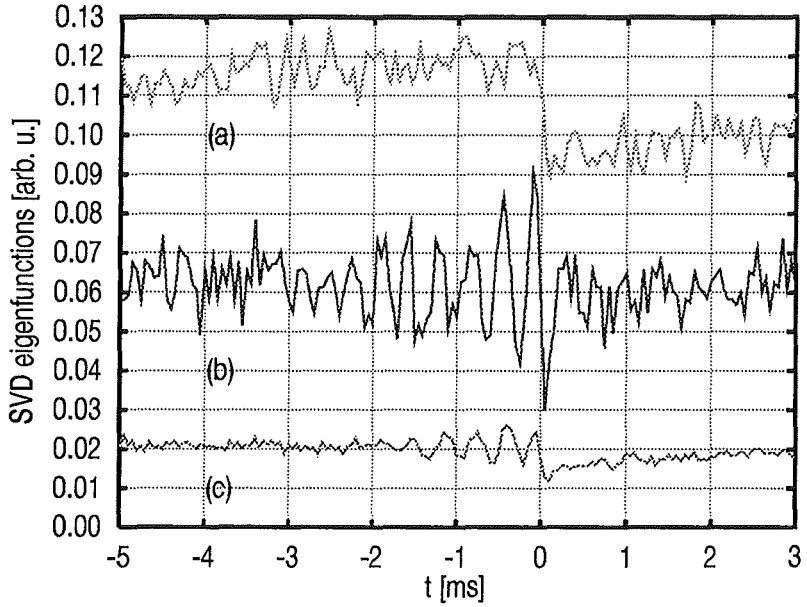
SVD eigenfunctions [arb. u.]
0.13
0.12
0.11
0.10
0.09
0.08
0.07
0.06
0.05
0.04
0.03
0.02
0.01
0.00
(a)
(b)
(c)
-5
-4
-3
-2
-1
0
1
2
3
t [ms]

Fig. 3

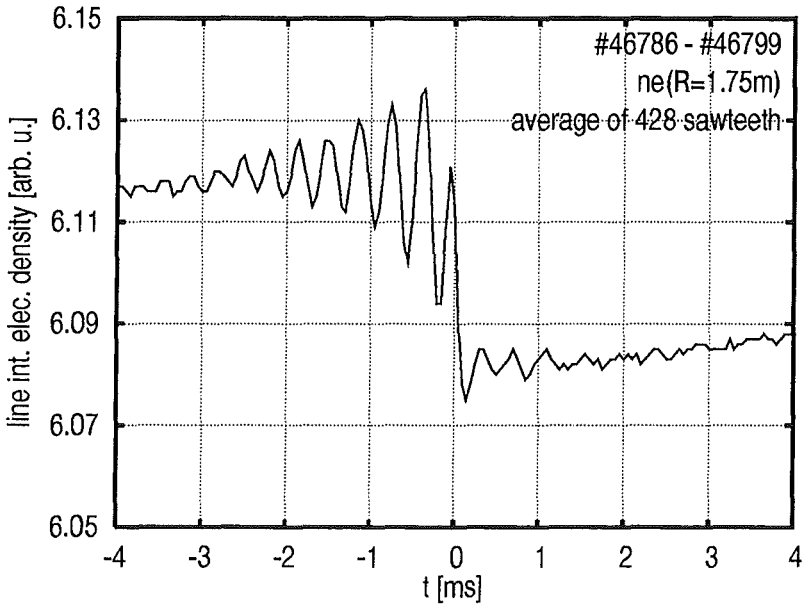
line int. elec. density [arb. u.]
6.15
6.13
6.11
6.09
6.07
6.05
#46786 - #46799
ne(R=1.75m)
average of 428 sawteeth
-4
-3
-2
-1
0
1
2
3
4
t [ms]

Fig. 4

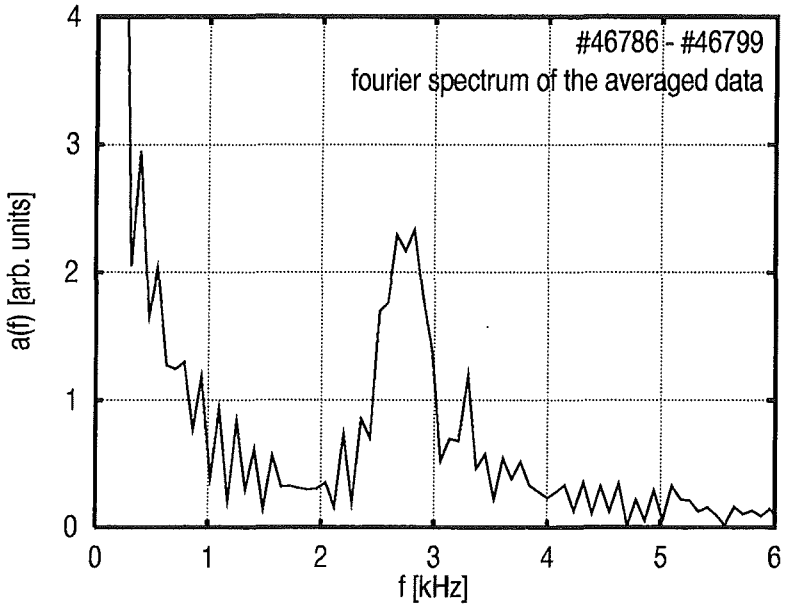
#46786 - #46799
fourier spectrum of the averaged data
a(f) [arb. units]
f [kHz]
0
1
2
3
4
5
6

Fig. 5

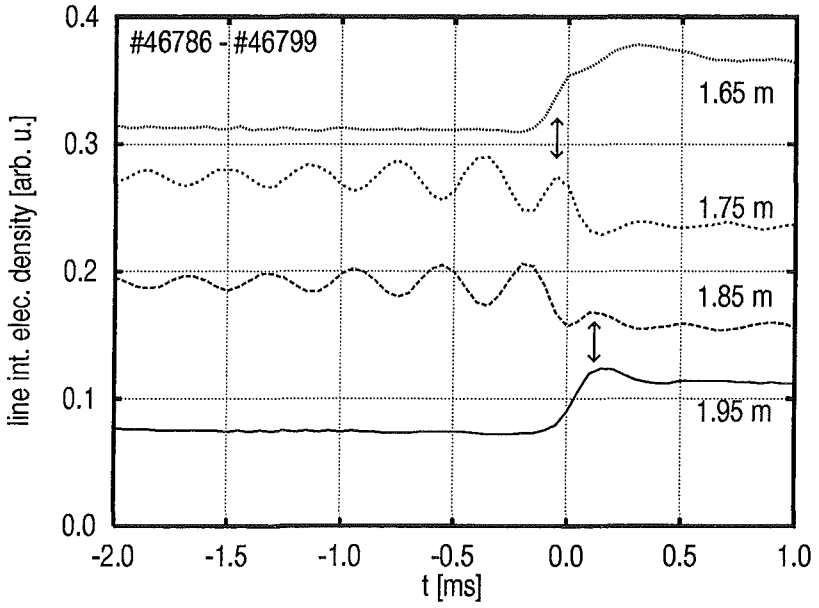
#46786 - #46799
1.65 m
1.75 m
1.85 m
1.95 m
line int. elec. density [arb. u.]
t [ms]
0.0
0.1
0.2
0.3
0.4
-2.0
-1.5
-1.0
-0.5
0.0
0.5
1.0

Fig. 6

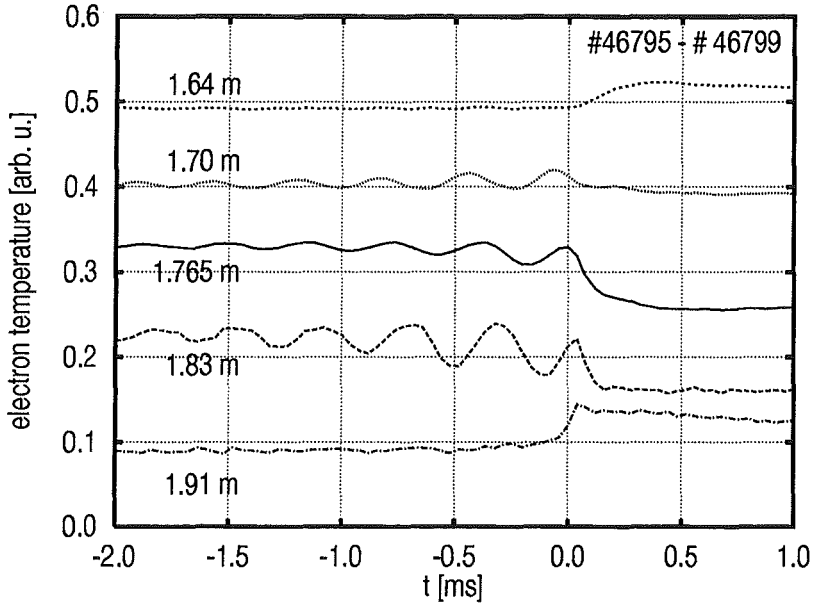
#46795 - # 46799
1.64 m
1.70 m
1.765 m
1.83 m
1.91 m
electron temperature [arb. u.]
t [ms]
0.0
0.1
0.2
0.3
0.4
0.5
0.6
-2.0
-1.5
-1.0
-0.5
0.0
0.5
1.0

Fig. 7

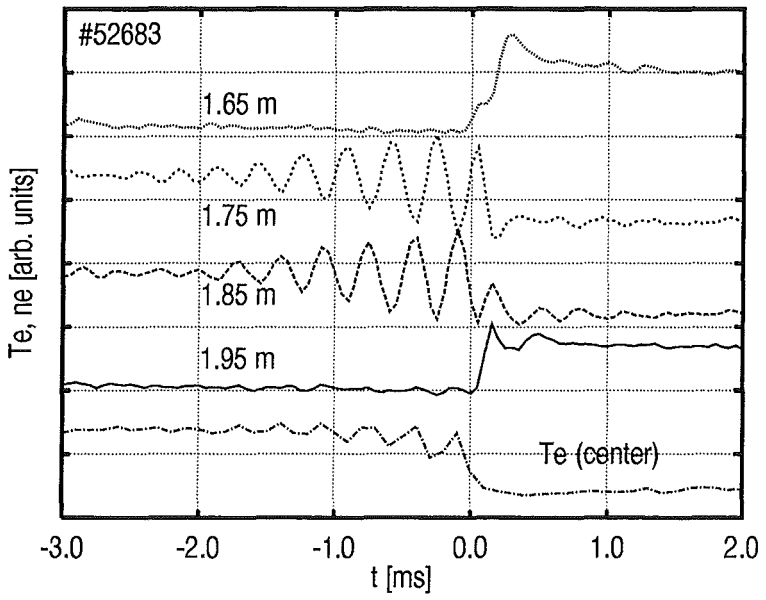
#52683
1.65 m
1.75 m
1.85 m
1.95 m
Te (center)
Te, ne [arb. units]
t [ms]
-3.0
-2.0
-1.0
0.0
1.0
2.0

Fig. 8

FORSCHUNGSZENTRUM JÜLICH GmbH

KFA

Jül-3114
September 1995
ISSN 0944-2952